# Surface charge induced modifications of the structure and dynamics of mixed dipolar liquids at solid–liquid interfaces: A molecular dynamics simulation study

Sanjib Senapati and Amalendu Chandra

Citation: The Journal of Chemical Physics **113**, 8817 (2000); doi: 10.1063/1.1318773
View online: http://dx.doi.org/10.1063/1.1318773
View Table of Contents: http://scitation.aip.org/content/aip/journal/jcp/113/19?ver=pdfcov
Published by the AIP Publishing

# Surface charge induced modifications of the structure and dynamics of mixed dipolar liquids at solid–liquid interfaces: A molecular dynamics simulation study

Sanjib Senapati and Amalendu Chandra
*Department of Chemistry, Indian Institute of Technology, Kanpur, U.P., India 208016*

(Received 16 May 2000; accepted 23 August 2000)

Molecular dynamics simulations are carried out to investigate the structural and dynamical properties of binary Stockmayer liquids near charged solid surfaces at varying surface charge density. The two solvent components differ widely in their polarity. The dipolar mixtures are formed at varying composition and the properties of the interfacial molecules are calculated in terms of several equilibrium and dynamical quantities such as the number density and polarization profiles, electrostriction at surfaces, linear and angular velocity autocorrelation functions, perpendicular ($z$) and parallel ($x,y$) components of translational diffusion tensors and rotational diffusion coefficients. The extent of selective adsorption of one species against the other at the surfaces is investigated as a function of surface charge density and composition and its effects on translational and rotational diffusion of interfacial molecules are discussed. The dynamical properties of the interfaces are also compared with those of the bulk. © *2000 American Institute of Physics.*
[S0021-9606(00)51143-X]

## I. INTRODUCTION

An understanding of the changes in structural and dynamical properties of dipolar solvents under the influence of surface charges is important in electrochemistry, biochemistry and surface science. Examples of such systems include polar solvents near charged electrodes, colloids, membranes, and macromolecules. In recent years, a considerable amount of work has been carried out on the properties of pure dipolar liquids in the vicinity of charged surfaces by means of experiments,[1–4] computer simulations[5–9] and analytical theories.[10–22] These studies have provided valuable information about the perturbation of the structure and dynamics of dipolar molecules caused by charged surfaces.

Toney *et al.*[2,3] investigated the interfacial structure of water molecules near charged metal surfaces by using *in situ* x-ray scattering experiments. They found that water is ordered in layers extending up to three molecular diameters and the orientation of interfacial water molecules depends on the sign of the charge density of the surfaces. More importantly, it was concluded from an analysis of their experimental data that the areal density of water next to a charged surface is very high compared to its bulk density. For example, according to Toney *et al.*,[2] the surface density of water molecules next to a positively charged silver electrode with a potential of 0.52 V (relative to the potential of zero charge on the electrode) is about two times as large as that of bulk water. Because of this molecular layering and high density, it was suggested that the dynamics of water molecules near charged surfaces would also be very different from the bulk molecules. However, a direct experimental measurement of the water dynamics in the vicinity of charged surfaces is yet to be carried out.

Computer simulations provide powerful methods to investigate the structural and dynamical properties of interfaces which otherwise are very difficult to study by means of experiments. Zhu *et al.*[5] carried out molecular dynamics (MD) simulations of water confined between two charged surfaces. They employed the so-called SPC–FP model of water and the surfaces were considered to be planar and uniformly charged. The water molecules near the charged surfaces were found to be ordered in layers in agreement with experimental observations. However, no significant increase of the density of water at the surfaces was observed. Also, the charge density of the surfaces was found to modify the hydrogen bond network through alignment of water molecules along the electric field generated by surface charge density. The external field was found to crowd the particle distribution along field direction inhibiting diffusion whereas it was found to play opposite role in the orthogonal directions. The structure of water near charged surfaces was also studied by Berkowitz and co-workers.[6] These authors carried out MD simulations of both nonpolarizable SPC/E[23] and polarizable PPC[24] models of water near charged metal surfaces and found no dramatic increase of the water density and disruption of hydrogen bonding near the charged surfaces. Thus, the huge increase of water density at a charged surface as concluded by Toney *et al.*[2] has not yet been confirmed by simulation results. Recently, Kiselev *et al.*[25] carried out a simulation study of SPC/E water in bulk under an external field. They found that self-diffusion coefficient strongly decreases with increasing electric field. However, no difference between the self-diffusion coefficients for motion parallel and perpendicular to the external field was detected in their study.

Patey and co-workers[10,11] investigated the equilibrium structure of model dipolar liquids near charged surfaces by employing integral equation theory and found layering of liquid molecules near the surfaces. The structure of dipolar

 

liquids near charged surfaces was also investigated by using density functional theory and Monte Carlo simulations.[15–21] It was shown that nonlinear phenomena like electrostriction and dielectric saturation could be rather significant for dipolar liquids near highly charged surfaces.[21] The extent of reorientation and also the surface-solvent correlation as evident from the maximum of the density profiles near a surface were found to increase nonlinearly with the surface charge density although no enormous increase of the areal density of solvent molecules at the charged surfaces was observed. A very recent study investigated the dynamics of solvent relaxation at solid–liquid interfaces by employing time dependent density functional theory.[22] The orientational relaxation of the interfacial dipolar molecules was found to occur at a somewhat slower rate.

While a large amount of work has been carried out for pure dipolar liquids near charged surfaces, much less effort has been devoted to examine dipolar mixtures at solid–liquid interfaces. Recently, Senapati and Chandra[26] investigated the structure of mixed dipolar liquids near charged solid surfaces by using density functional theory and Monte Carlo simulations. The dynamics of polarization relaxation in a dipolar mixture near a newly charged solid surface has also been studied by using time dependent density functional theory.[27] These authors have also carried out molecular dynamics simulations of mixed Stockmayer liquids near uncharged surfaces to investigate the role of selective adsorption in determining the equilibrium and dynamical properties of mixed dipolar liquids at hydrophobic surfaces.[28] However, until now no molecular dynamics simulation has been carried out to study the dynamics of mixed dipolar liquids near charged surfaces. Thus, the surface charge induced modifications of selective adsorption at varying composition and surface charge density and its effects on translational and orientational motion of interfacial molecules have not yet been investigated. Clearly, there remains a need to carry out a detailed molecular dynamics simulation of mixed dipolar liquids at varying composition and surface charge density in order to understand the equilibrium and dynamical properties of such complex interfaces at molecular level. Such a study is presented in this work.

Our goal in the present work has been to take a simple model for dipolar mixtures near charged solid surfaces and study its structure and dynamics in a detailed manner. From molecular dynamics point of view, binary mixtures of Stockmayer liquids of different polarity near uniformly charged planar surfaces seem to be simple systems for studying the dependence of equilibrium and dynamical properties of dipolar mixtures at solid–liquid interfaces on composition and surface charge density. The two dipolar components considered in the present study differ largely in their polarity. The surfaces are uniformly charged and, therefore, act as hydrophilic surfaces. We have simulated five different mixtures of varying composition and for each mixture we have considered three different values of the surface charge density. Thus, altogether we have simulated 15 different interfacial systems. The presence of the charged surfaces makes the systems inhomogeneous and anisotropic. The extent of such inhomogeneity and anisotropy is investigated by calculating the number density and polarization profiles of both the components next to the solid surfaces. The dynamical properties of the dipolar mixtures near surfaces are studied by calculating the linear and angular velocity autocorrelation functions and the translational and rotational diffusion coefficients of both the species.

The outline of the rest of the paper is as follows. The basic model and simulation details are described in Sec. II. In Sec. III, we present the results of the inhomogeneous spatial and orientational structure of the dipolar mixture next to the charged surfaces at varying composition. The results of the dynamical properties are discussed in Sec. IV and our conclusions are summarized in Sec. V.

## II. THE MODEL AND SIMULATION DETAILS

We have carried out molecular dynamics simulations of five different mixtures consisting of binary dipolar liquids of varying composition. The dipolar mixtures are confined between two planar surfaces which are either charged or uncharged. For each of the five mixtures we have considered three different values of the surface charge density. Thus, altogether we have simulated 15 different systems. The solvent molecules interact with each other through a spherically symmetric short-range potential and an anisotropic long-range electrostatic potential and they also interact with the two surfaces. The total configurational energy of the system can be expressed in the form

$$U=\frac{1}{2}\sum_{\alpha,\beta=1}^{2}\sum_{i=1}^{N_\alpha}\sum_{j=1}^{N_\beta}u_{\mathrm{SR}}^{\alpha\beta}(r_{ij})-\frac{1}{2}\sum_{\alpha=1}^{2}\sum_{i=1}^{N_\alpha}\mu_i^\alpha\cdot E_i^\alpha+\sum_{\alpha=1}^{2}U_{w\alpha}, \tag{1}$$

where $N_\alpha$ is the number of molecules of species $\alpha$, $r_{ij}$ is the distance between molecule $i$ of species $\alpha$ and molecule $j$ of species $\beta$ and $E_i^\alpha$ is the electric field at molecule $i$ of species $\alpha$ due to all other dipoles in the system. $\mu_i^\alpha$ is the dipole vector (of magnitude $\mu_\alpha$) of $i$th molecule of species $\alpha$. We follow the standard convention for the direction of a dipole moment vector in which the dipole moment points from the negative end to the positive end of a molecule. $u_{\mathrm{SR}}^{\alpha\beta}(r_{ij})$ is the spherically symmetric short-range interaction which is taken to be the Lennard-Jones potential

$$u_{\mathrm{SR}}^{\alpha\beta}(r_{ij})=4\epsilon_{\alpha\beta}[(\sigma_{\alpha\beta}/r_{ij})^{12}-(\sigma_{\alpha\beta}/r_{ij})^{6}]. \tag{2}$$

In Eq. (2), $\sigma_{\alpha\beta}=0.5(\sigma_\alpha+\sigma_\beta)$ and $\epsilon_{\alpha\beta}=\sqrt{\epsilon_\alpha\epsilon_\beta}$ where $\sigma_\alpha$ and $\epsilon_\alpha$ are, respectively, the Lennard-Jones diameter and well-depth parameter of solvent molecules of species $\alpha$. The first two terms of Eq. (1) constitute the so-called Stockmayer potential. The third term in Eq. (1) arises from the interaction of solvent molecules with the two planar walls. We assume that the walls are uniformly charged, and are located at positions $-z_0$ and $z_0$ along the $z$ axis and $x$ and $y$ axes are parallel to the surfaces. For this geometry, the wall-solvent interaction potential can be described as a function of the $z$ coordinate of particle $i$ and $U_{w\alpha}$ can be written as

$$U_{w\alpha}=\sum_{i=1}^{N_\alpha} u_{w\alpha}(|z_i^\alpha+z_0|)+\sum_{i=1}^{N_\alpha} u_{w\alpha}(|z_i^\alpha-z_0|), \tag{3}$$

where $u_{w\alpha}(|z_i^\alpha-z_0|)$ is the interaction of $i$th solvent molecule of species $\alpha$ with the surface located at $z_0$. This interaction includes a short-range isotropic part and a Coulombic anisotropic part. The short-range isotropic part does not depend on dipole orientation and it can be described by a 9–3 potential.[29,30] The Coulombic part is the interaction of a dipole with a uniform field generated by the surface charge density. Thus, we write $u_{w\alpha}(z)$ in the following form:

$$u_{w\alpha}(z)=\frac{3^{3/2}\epsilon_{w\alpha}}{2}\left[\left(\frac{\sigma_{w\alpha}}{z}\right)^9-\left(\frac{\sigma_{w\alpha}}{z}\right)^3\right]-E(z)\cdot\mu_i^\alpha, \tag{4}$$

where $z=|z_i^\alpha-z_0|$ and $\epsilon_{w\alpha}$ and $\sigma_{w\alpha}$ are the well-depth parameter and diameter which characterize the short-range part of the wall-solvent interaction between a solid wall and a molecule of species $\alpha$. $E(z)$ is the electric field generated by the surface charge density. The validity of this uniform field in the context of real interfacial systems is discussed in Sec. V. In the present simulations the wall located at $-z_0$ is assumed to have a positive charge density $\sigma_c$ and the one at $z_0$ is assigned a negative charge density of equal magnitude. This generates a uniform field of magnitude $4\pi\sigma_c$ across the system. The forces and torques on particle $i$ caused by its interaction with the charged wall can be readily calculated.

The simulations were carried out in rectangular boxes of dimensions $L\times L\times h$ where $h$ is the separation between the surfaces which is defined to be the distance between the two wall origins and $L$ is the length of the central simulation box in $x$ and $y$ directions. Periodic boundary conditions were employed in the $x$ and $y$ directions. In the present simulations, the solvent molecules of different species are assumed to have the same mass $m$ and also the same Lennard-Jones parameters such that $\sigma_1=\sigma_2=\sigma$, $\epsilon_1=\epsilon_2=\epsilon$ and also $\sigma_{w1}=\sigma_{w2}=\sigma_w$ and $\epsilon_{w1}=\epsilon_{w2}=\epsilon_w$. However, the molecules of the two species have different dipole moments. With the above simplifications, the systems studied here can be completely specified by specifying the values of $L$ and $h$, the number of particles $N_\alpha$, the reduced dipole moment $\mu_\alpha^*=\sqrt{\mu_\alpha^2/\epsilon\sigma^3}$, reduced moment of inertia $I_\alpha^*=I_\alpha/m\sigma^2$, the reduced temperature $T^*=k_BT/\epsilon$, the reduced surface charge density $\sigma_c^*=\sigma_c\sqrt{\sigma^3/\epsilon}$ and the reduced wall-solvent interaction parameters: $\epsilon_w^*=\epsilon_w/\epsilon$ and $\sigma_w^*=\sigma_w/\sigma$ where $k_B$ is Boltzmann constant. The reduced number density of species $\alpha$ is $\rho_\alpha^*$ which is equal to $\rho_\alpha\sigma^3$. For all the systems, we have taken $\epsilon_w^*=3$ and $\sigma_w^*=0.8$. We note that these values of the reduced wall-solvent interaction parameters fall in the realistic range. In the calculations, we have used three different values of surface charge density: $\sigma_c^*=$ 0.0, 0.28, and 0.56. The values of the other parameters characterizing the five mixtures considered in this study are summarized in Table I. The simulations were carried out with a total of 256 molecules.

The MD simulations were carried at constant temperature employing the leap-frog algorithm with a reduced time step $\Delta t^*=\Delta t(\epsilon/m\sigma^2)^{1/2}=0.0025$. The quaternion formulation was employed for the rotational motion.[31] For all the systems, the wall origins are located at $z=0$ and $z=10\sigma$ and periodic boundary conditions are set at $x,y=0$ and $6.17\sigma$ in $x$ and $y$ directions. The long-range electrostatic interactions were treated by using the slab adapted Ewald summation method as proposed by Shelley and Patey.[32] In this method, the slabs of dipolar liquid are separated by a region which contains no dipolar molecules and has a dielectric constant of 1. The periodicity of the system in $z$ direction is $25.4\sigma$ for all the systems which correspond to having an empty region of about $15\sigma$ between the slabs of dipolar molecules. We have verified that the surfaces are sufficiently far apart that the interactions between the slabs are negligible. The Ewald parameters employed were $\alpha/L=6.4$, a reciprocal space cut off of $15\sigma^{-1}$ and $\epsilon'=\infty$. The minimum image convention was used for real space portion of the Ewald sum. All the systems were equilibrated for at least 100 000 time steps before production runs for a minimum of 500 000 time steps were started. The results of the various equilibrium and dynamical properties of the two components at interfaces and in the bulk phases for different surface charge density are presented in the following sections.

TABLE I. Values of different parameters.

| Mixture | $N_1$ | $N_2$ | $x_1$[a] | $\mu_1^*$ | $\mu_2^*$ | $I^*$ | $T^*$ |
|---|---|---|---|---|---|---|---|
| 1 | 256 | 0 | 1.0 | 1.8 | 0.75 | 0.025 | 1.35 |
| 2 | 192 | 64 | 0.75 | 1.8 | 0.75 | 0.025 | 1.35 |
| 3 | 128 | 128 | 0.50 | 1.8 | 0.75 | 0.025 | 1.35 |
| 4 | 64 | 192 | 0.25 | 1.8 | 0.75 | 0.025 | 1.35 |
| 5 | 0 | 256 | 0.0 | 1.8 | 0.75 | 0.025 | 1.35 |

[a]$x_1$ is the mole fraction of species 1.

## III. STRUCTURAL PROPERTIES

We have examined the effects of charged surfaces on the number density and polarization profiles of dipolar molecules. The density profiles of the two species are calculated by computing the average number of molecules in slabs of thickness $\Delta z=0.02\sigma$ lying on either sides of the central plane at $z=0$. The effects of charged surfaces on the polarization of dipolar molecules of different species are determined by calculating the wall-solvent correlation function $g_{w\alpha}(z,\theta)$ where $\theta$ is the angle between the dipole vector of a molecule of species $\alpha$ and the surface normal. For convenience, we expand $g_{w\alpha}(z,\theta)$ in the basis set of Legendre polynomials as follows:

$$g_{w\alpha}(z,\theta)=\sum_l (-1)^l g_{w\alpha}^{0ll}(z)P_l(\cos\theta), \tag{5}$$

where $P_l(\cos\theta)$ is the Legendre polynomial of order $l$. Clearly, $\rho_\alpha g_{w\alpha}^{000}(z)$ gives the number density of the solvent species $\alpha$ next to the solid surfaces where $\rho_\alpha$ is the corresponding average (or bulk) density. $g_{w\alpha}^{0ll}(z)$ for $l\neq 0$ gives information about the orientational structure of dipolar molecules near the surfaces. For the present model, $g_{w\alpha}^{011}(z)$ is the most important orientational term and is related to $z$ component of the polarization of species $\alpha$, $P_\alpha(z)$, by the following relation:

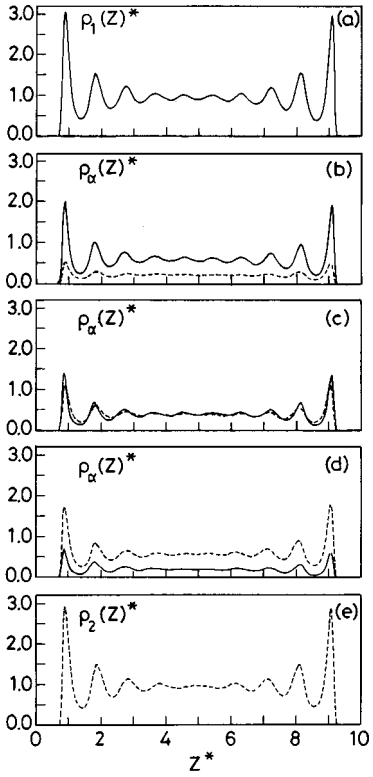


FIG. 1. The position dependence of inhomogeneous number density of the two components for (a) mixture 1, (b) mixture 2, (c) mixture 3, (d) mixture 4 and (e) mixture 5. The surface charge density $\sigma_c^*=0.56$. The solid and dashed curves are for species 1 and 2, respectively. The reduced number density $\rho_\alpha(z)^* = \rho_\alpha(z)\sigma^3$ and the reduced distance $z^*=z/\sigma$ where $\sigma$ is the molecular diameter.

$$P_\alpha(z) = -\frac{2\mu_\alpha\rho_\alpha}{3} g_{w\alpha}^{011}(z). \tag{6}$$

We note that the $x$ and $y$ components of the polarization are zero for both the species for all the systems considered in this work.

In Fig. 1 we have shown the number density $\rho_\alpha(z)^*$ of both the components as a function of distance from the two surfaces at a given surface charge density $\sigma_c^*=0.56$. The results are shown for all the five mixtures of varying composition. The density profiles are seen to be highly nonuniform near the solid surfaces. Also, for the equimolar mixture, the height of the maximum of the number density profile of the more polar species at the surfaces is found to be higher than that of the less polar species. This implies a stronger wall-solvent correlation of the more polar molecules at the charged surfaces. This enhanced wall-solvent correlation of the more polar component at the charged surfaces is also evident in the density profiles of other systems of different mole fractions.

In Figs. 2 and 3, we show the results of the field dependence of the density changes $\Delta\rho_\alpha(z)$ $[\Delta\rho_\alpha(z)=\rho_\alpha(z;\sigma_c) - \rho_\alpha(z;\sigma_c=0)]$ of both the species. It is seen that in case of mixtures the density of the more polar species near the surface increases whereas that of the less polar species decreases with increasing surface electrostatic field. The increase or decrease of solvent density near a charged surface

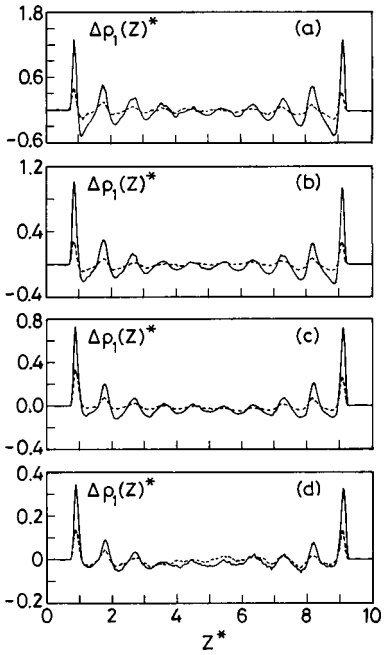


FIG. 2. The variation of change in number density $\Delta\rho_1(z)^*$ $[=\rho_1(z;E) - \rho_1(z;E=0)]$ for species 1 with distance from the charged surfaces for (a) mixture 1, (b) mixture 2, (c) mixture 3, (d) mixture 4. The solid and dashed curves are for $\sigma_c^*=0.56$ and 0.28, respectively.

is a measure of the electrostriction caused by the charge density of the surfaces. Thus, with increasing surface charge density, the more polar species shows a positive electrostriction and the less polar species shows a negative electrostriction. This implies a selective adsorption of the more polar molecules at the surface with increasing surface charge den-

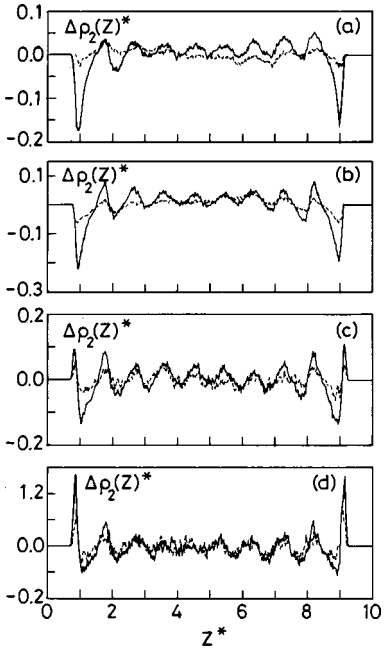


FIG. 3. The variation of change in number density $\Delta\rho_2(z)^*$ $[=\rho_2(z;E) - \rho_2(z;E=0)]$ for species 2 with distance from the charged surfaces for (a) mixture 2, (b) mixture 3, (c) mixture 4, (d) mixture 5. The solid and dashed curves are for $\sigma_c^*=0.56$ and 0.28, respectively.

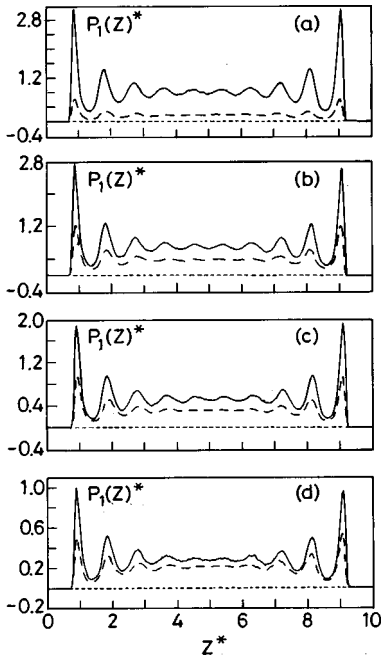


FIG. 4. The variation of reduced polarization of species 1 with distance from the charged surfaces for (a) mixture 1, (b) mixture 2, (c) mixture 3, (d) mixture 4. The solid, long-dashed, and the short-dashed curves are for $\sigma_c^* = 0.56$, 0.28, and 0.0, respectively. Note that the short-dashed curve is essentially a straight line as the polarization near an uncharged surface is zero within very small statistical error.

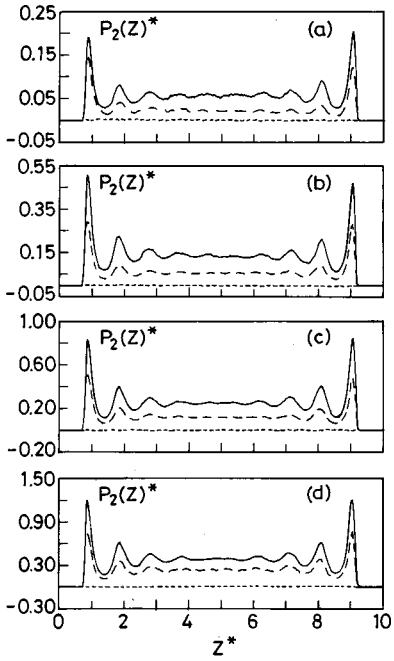


FIG. 5. The variation of reduced polarization of species 2 with distance from the charged surfaces for (a) mixture 2, (b) mixture 3, (c) mixture 4, (d) mixture 5. The different curves are as in Fig. 4.

sity. The extent of the selective adsorption at a charged surface can also be studied by calculating the changes of the number of solvent molecules of the two species ($\Delta n_\alpha$) in the first interfacial layer with changes of the surface charge density. Note that $\Delta n_\alpha = n_\alpha(\sigma_c) - n_\alpha(\sigma_c = 0)$ where $n_\alpha$ is the number of molecules of species $\alpha$ in the contact interfacial layer near a surface. We have calculated $\Delta n_\alpha$ by integrating the density profiles from $z = 0$ to the distance of the first density minimum for $\sigma_c = 0$ and also for $\sigma_c = 0.28$ and 0.56. It is found that for $\sigma_c = 0.56$, $\Delta n_1 = 1.85$, and $\Delta n_2 = -2.2$ for mixture 2, $\Delta n_1 = 2.7$ and $\Delta n_2 = -3.3$ for mixture 3 and $\Delta n_1 = 1.8$, $\Delta n_2 = -1.9$ for mixture 4. The positive values of $\Delta n_1$ and the negative values of $\Delta n_2$ clearly reveal the presence of selective adsorption of the more polar molecules at the charged surfaces.

The results of the polarization profiles of the two components are shown in Figs. 4 and 5. For charged surfaces, the polarizations are found to be most significant near the surfaces and then they oscillate until bulk values are reached. The range of oscillations increases with increase of the surface electric field and it is more pronounced for the more polar species. The orientational order of the interfacial molecules is found to change nonlinearly with the surface charge density and also with the composition of the mixture. The nonzero polarization profiles of Figs. 4 and 5 show that the dipolar molecules prefer to orient perpendicular to the charged surfaces. For the uncharged surfaces, there is no net polarization. In fact, the statistical error in the polarization profiles for uncharged surfaces is extremely small and thus the expected zero polarization for these systems is reproduced quite accurately. Although there is no preferred orientation of dipolar molecules near uncharged surfaces, a calculation of $g_{w\alpha}^{022}(z)$ reveals that the dipolar molecules tend to align parallel to the uncharged surfaces, in agreement with the results of earlier studies.[28,33,34]

## IV. DYNAMIC PROPERTIES

We report the various dynamical properties of the dipolar mixtures near the charged surfaces that have been studied in this work. Our primary goal is to investigate the effects of surface charge density on dynamics of the dipolar mixture in the interfacial region. We are also interested to see to what extent the dynamics of interfacial molecules differ from that in the bulk phase under the same external field. We have computed the velocity and angular velocity autocorrelation functions and from these correlation functions we have calculated the translational and rotational diffusion coefficients. The above dynamical quantities are calculated as functions of surface charge density and composition of the dipolar mixture. The spatial structures shown in the preceding section reveal that the dipolar mixtures are highly inhomogeneous near the two surfaces. To compare the dynamical properties of the interfacial medium with those of the bulk liquid, we have divided the entire system into three regions. The region I (or the interfacial region) consists of molecules which are within the distance of first minimum of the density distributions from the two solid surfaces, region II (or the diffuse interfacial region) includes particles lying between the first and third minima of the number density profile, and the rest is region III (or the bulk region).

We denote the $i$th component of velocity of a dipolar molecule of species $\alpha$ by $v_\alpha^i(t)$ and its normalized autocorrelation function $C_{v,\alpha}^i(t)$ is defined by[35]

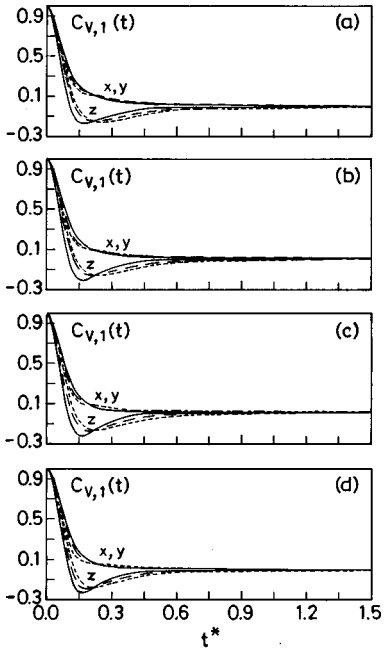


FIG. 6. The time dependence of the perpendicular ($z$) and parallel ($x,y$) components of velocity autocorrelation functions for species 1 for (a) mixture 1, (b) mixture 2, (c) mixture 3, (d) mixture 4. The results are for the interfacial region I. The different curves are as in Fig. 4.

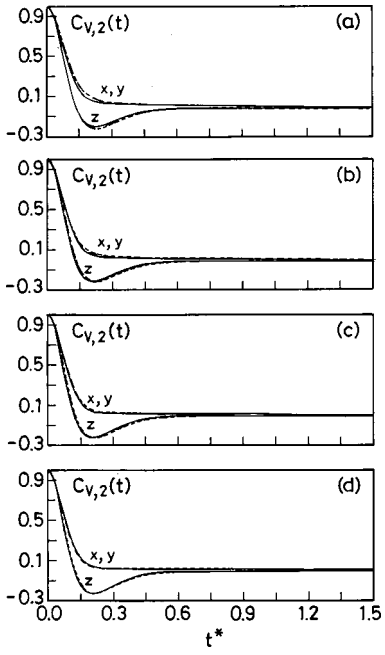


FIG. 7. The time dependence of the perpendicular ($z$) and parallel ($x,y$) components of velocity autocorrelation functions for species 2 for (a) mixture 2, (b) mixture 3, (c) mixture 4, (d) mixture 5. The results are for the interfacial region I. The different curves are as in Fig. 4.

$$C^i_{v,\alpha}(t)=\frac{\langle v^i_\alpha(t)v^i_\alpha(0)\rangle}{\langle v^i_\alpha(0)^2\rangle}, \tag{7}$$

where $i=x,y,z$ and $\alpha=1,2$ and $\langle\cdots\rangle$ represents an equilibrium ensemble average. Because of the presence of wall-solvent interaction, the system is anisotropic and, therefore, diffusion is not isotropic. This is illustrated in Figs. 6 and 7 where we have shown the decay of parallel ($x,y$) and perpendicular ($z$) components of velocity–velocity autocorrelation functions for the interfacial dipolar molecules for different values of the surface charge density. In Fig. 6, we have shown the results for species 1 and the results for species 2 are shown in Fig. 7. In both the figures, the two velocity components are seen to decay differently. Clearly, diffusion along the parallel direction is expected to be quite different from that in the perpendicular direction. Also, the external electric field is found to accelerate the velocity relaxation along the $z$ direction whereas the opposite effect is observed for the relaxation along $x,y$ directions. This enhanced and reduced rates of velocity relaxation in the perpendicular and parallel directions, respectively, are most pronounced for species 1 because of its higher polarity.

The translational diffusion coefficient $D^i_\alpha$ ($i=x,y,z$ and $\alpha=1,2$) can be calculated from the velocity–velocity autocorrelation function of species $\alpha$ by using the following relation[35]

$$D^i_\alpha=\frac{k_BT}{m}\int_0^\infty C^i_{v,\alpha}(t)dt. \tag{8}$$

We note that the self-diffusion coefficient, as defined by Eq. (8), includes the influence of the external field because the relaxation of the velocity–velocity autocorrelation function depends on the strength of the external field. The above definition of the self-diffusion coefficient is different from the one which uses the concept of a field-free diffusion coefficient and includes the effects of external field by incorporating an additional term in the relaxation equation. The present terminology of field dependent diffusion coefficient has the advantage that it helps to make a direct comparison of the relative rates of relaxation in absence and in presence of an external field. We also note that the terminology of field dependent diffusion coefficient was also used in previous simulation studies of dynamical properties of water under external fields.[25,36]

We have calculated $D^{x,y}_\alpha$ and $D^z_\alpha$ for interfacial and bulk regions for all the systems and the results are shown in Table II. The standard deviations associated with the average values vary from 2 to 8 percent of the reported values for both the species. The standard deviations are determined by dividing the total run period into blocks of 50 000 time steps and treating the block averages as independent estimates of the time correlation functions and diffusion coefficients. It is seen that the perpendicular diffusion near the surfaces is hindered and the parallel diffusion is enhanced compared to diffusion in the bulk mixture. Also, with increase of surface charge density, the perpendicular diffusion of interfacial molecules is further slowed down and the parallel diffusion is enhanced. The results of the diffuse interfacial region (region II) are not very different from the bulk results[37] and, therefore, are not included here. We note that the forces from the surfaces act only along the $z$ direction and this leads to slowing down of diffusion along the perpendicular direction. The solvent molecules in the interfacial region feel a less effective friction for motion along $x$ and $y$ direction since there are no solvent molecules on the surface sides of the

TABLE II. Translational diffusion coefficients of species 1 and 2 for all the five mixtures at three different values of the surface charge density.[a]

| | | Interface | | | Bulk | | |
|---|---|---|---|---|---|---|---|
| Quantity | Mixture | $\sigma_c^*=0.0$ | 0.28 | 0.56 | $\sigma_c^*=0.0$ | 0.28 | 0.56 |
| $D_1^{z*}$ | 1 | 0.0102 | 0.0100 | 0.0084 | 0.1010 | 0.0919 | 0.0906 |
| | 2 | 0.0105 | 0.0103 | 0.0086 | 0.0890 | 0.0862 | 0.0770 |
| | 3 | 0.0110 | 0.0103 | 0.0092 | 0.0881 | 0.0828 | 0.0719 |
| | 4 | 0.0111 | 0.0107 | 0.0096 | 0.0819 | 0.0780 | 0.0685 |
| $D_1^{x,y*}$ | 1 | 0.1501 | 0.1623 | 0.1655 | 0.0962 | 0.1166 | 0.1229 |
| | 2 | 0.1462 | 0.1601 | 0.1645 | 0.0893 | 0.1139 | 0.1221 |
| | 3 | 0.1402 | 0.1454 | 0.1566 | 0.0881 | 0.1134 | 0.1145 |
| | 4 | 0.1331 | 0.1407 | 0.1527 | 0.0822 | 0.1121 | 0.1139 |
| $D_2^{z*}$ | 2 | 0.0081 | 0.0039 | 0.0037 | 0.0941 | 0.0930 | 0.0907 |
| | 3 | 0.0091 | 0.0055 | 0.0051 | 0.0921 | 0.0904 | 0.0892 |
| | 4 | 0.0102 | 0.0068 | 0.0062 | 0.0881 | 0.0872 | 0.0843 |
| | 5 | 0.0145 | 0.0140 | 0.0131 | 0.0870 | 0.0863 | 0.0841 |
| $D_2^{x,y*}$ | 2 | 0.1561 | 0.1704 | 0.1791 | 0.0942 | 0.1183 | 0.1211 |
| | 3 | 0.1541 | 0.1631 | 0.1675 | 0.0920 | 0.1175 | 0.1196 |
| | 4 | 0.1451 | 0.1560 | 0.1579 | 0.0901 | 0.1159 | 0.1161 |
| | 5 | 0.1301 | 0.1396 | 0.1436 | 0.0872 | 0.1136 | 0.1146 |

[a]$D_\alpha^*=D_\alpha(m/\epsilon\sigma^2)^{1/2}$ where $\alpha=1,2$.

interfaces and this leads to increased values of $D_\alpha^{x,y}$ for interfacial molecules. This is also clear from Figs. 8 and 9 where we have shown the time dependence of the parallel and perpendicular components of velocity autocorrelation functions of interfacial and bulk molecules for a given surface charge density.

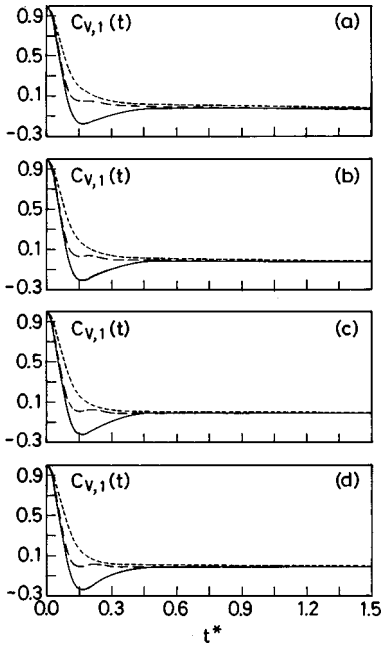


FIG. 8. The comparison of the relaxation of velocity autocorrelation functions of species 1 at interface and in the bulk phase for surface charge density $\sigma_c^*=0.56$. The solid and the short-dashed curves represent, respectively, the perpendicular ($z$) and parallel ($x,y$) components of the velocity autocorrelation function at interface. The long-dashed curve represents the decay of $C_v(t)$ in the corresponding bulk phase. (a), (b), (c), and (d) are for mixtures 1, 2, 3, and 4, respectively.

The rotational diffusion coefficients are calculated from the time correlation function of angular velocity by using the relation[35]

$$\Theta_\alpha=\frac{k_BT}{I_\alpha}\int_0^\infty C_{\omega,\alpha}(t)dt, \tag{9}$$

where $C_{\omega,\alpha}(t)$ is the normalized angular velocity autocorrelation function of species $\alpha$. We have calculated the angular

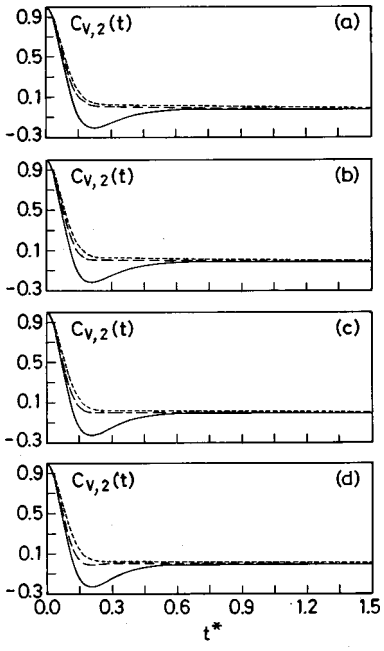


FIG. 9. The comparison of the relaxation of velocity autocorrelation functions of species 2 at interface and in the bulk phase for surface charge density $\sigma_c^*=0.56$. The different curves are as in Fig. 8. (a), (b), (c), and (d) are for mixtures 2, 3, 4, and 5, respectively.

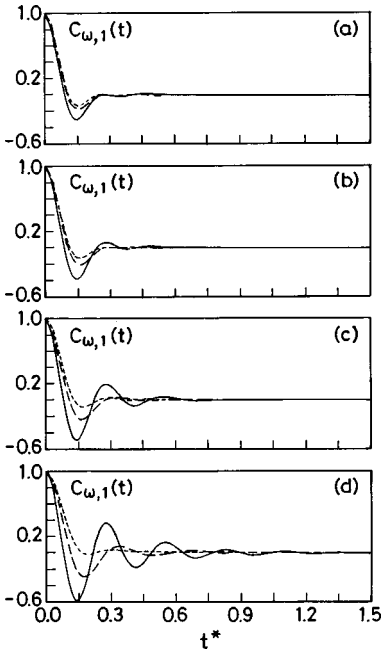


FIG. 10. The time dependence of the angular velocity autocorrelation function for species 1 for (a) mixture 1, (b) mixture 2, (c) mixture 3, (d) mixture 4. The results are for the interfacial region I. The different curves are as in Fig. 4.

velocity autocorrelation functions for interfacial and bulk molecules for both the species and the results are shown in Figs. 10–12. In Table III, we have included the values of rotational diffusion coefficients of the two species for varying composition and surface charge density. The standard deviations associated with the average values of rotational

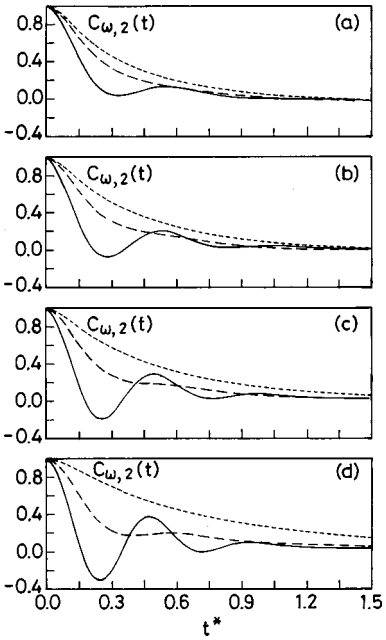


FIG. 11. The time dependence of the angular velocity autocorrelation function for species 2 for (a) mixture 2, (b) mixture 3, (c) mixture 4, (d) mixture 5. The results are for the interfacial region I. The different curves are as in Fig. 4.

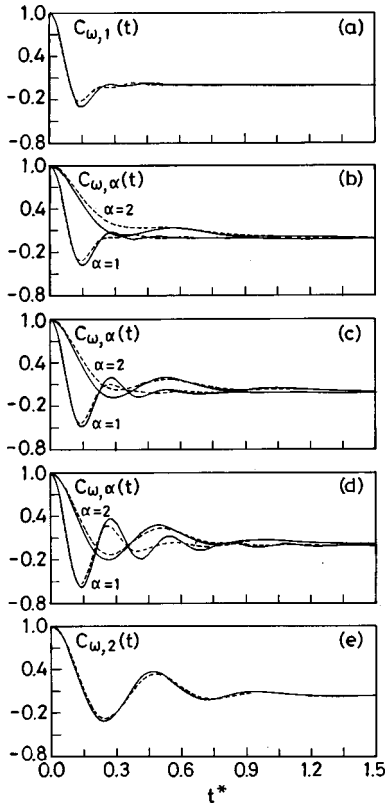


FIG. 12. The comparison of the relaxation of angular velocity autocorrelation functions at interface and in the bulk phase for species 1 and 2. The surface charge density $\sigma_c^* = 0.56$. The solid and the short-dashed curves are for the interfacial region and the bulk. (a), (b), (c), (d), and (e) are for mixtures 1, 2, 3, 4, and 5, respectively.

diffusion coefficients vary from 2 to 4 percent of the reported values. In case of uncharged surfaces, the rotational diffusion at the interface is found to occur at a slightly slower or almost identical rate (within statistical error) compared to that in the bulk phase for the pure liquid of the strongly polar component. However, when mixtures are formed by adding the weakly polar component, the rotational diffusion occurs at a faster rate near the surfaces than that in the bulk. This varying rotational diffusional behavior is an outcome of the combined effects of the orientational ordering imposed by the walls, a less torque acting on interfacial solvent molecules because of an incomplete solvation shell and selective adsorption of less polar molecules at the uncharged surfaces.

With increase of surface charge density, the rotational diffusion of both interfacial and bulk molecules occur at a slower rate. However, the extent of rotational slowing down is found to be more prominent for interfacial molecules relative to their values for $\sigma_c = 0$. For charged surfaces, the slowing down of the rotational diffusion of interfacial molecules compared to that of bulk molecules is observed for systems 1–3 which can be attributed to the selective adsorption of more polar component at the surfaces in these systems. This behavior is also clear in Figs. 10 and 11 where pronounced negative regions of the angular velocity autocorrelation functions are seen for charged surfaces. In systems 4 and 5, the rotational diffusion near a charged surface occurs at a slightly faster rate than that in the bulk phase even for $\sigma_c$

TABLE III. Rotational diffusion coefficients of species 1 and 2 for all the five mixtures at three different values of the surface charge density.[a]

| | | Interface | | | Bulk | | |
|---|---|---|---|---|---|---|---|
| Quantity | Mixture | $\sigma_c^*=0.0$ | 0.28 | 0.56 | $\sigma_c^*=0.0$ | 0.28 | 0.56 |
| $\Theta_1^*$ | 1 | 2.628 | 2.198 | 1.329 | 2.658 | 2.364 | 1.565 |
| | 2 | 2.764 | 1.998 | 1.011 | 2.670 | 2.164 | 1.086 |
| | 3 | 3.430 | 1.976 | 0.917 | 2.745 | 2.027 | 0.944 |
| | 4 | 4.490 | 1.963 | 0.904 | 3.150 | 1.849 | 0.807 |
| $\Theta_2^*$ | 2 | 20.84 | 17.17 | 11.41 | 17.74 | 17.65 | 13.65 |
| | 3 | 24.35 | 17.03 | 10.94 | 18.86 | 17.28 | 12.19 |
| | 4 | 28.96 | 16.92 | 9.813 | 21.28 | 16.87 | 9.712 |
| | 5 | 40.63 | 16.90 | 8.750 | 30.15 | 16.72 | 8.610 |

[a]$\Theta_\alpha^*=\Theta_\alpha(m\sigma^2/\epsilon)^{1/2}$ where $\alpha=1,2$.

$=0.56$ which can be attributed to the dominance of weakly polar molecules in the interfacial region for these two systems.

An interesting behavior is observed for the change of rotational diffusion with variation of composition. For the uncharged surfaces, the rotational diffusion of both the species increases with increase of mole fraction of the less polar species. This can be understood in terms of less polarity of the medium and hence less dielectric friction on rotation with increase of the number of less polar molecules. For finite charge density of the surfaces, an opposite behavior is observed. Now the rotational diffusion coefficients decrease with increasing mole fraction of the less polar molecules. This can be attributed to an interplay between the dipole–dipole and dipole–surface interactions. The effective interaction between solvent dipoles decreases with increase of the mole fraction of less polar species and because of this reduced effective dipole–dipole interaction, the surface electric field can perturb the rotational motion more effectively and this leads to a decrease of the rotational diffusion coefficients. This is more clear from the plots of angular velocity autocorrelations of Fig. 12 which show deeper negative regions with increase of the relative concentration of less polar molecules for $\sigma_c^*=0.56$.

## V. SUMMARY AND CONCLUSIONS

We have investigated the surface charge induced changes of the structure and dynamics of mixed dipolar liquids at solid–liquid interfaces by means of molecular dynamics simulations. The dipolar mixtures consist of a strongly polar and a weakly polar solvent. Fifteen different systems of varying composition and surface charges are investigated. Various structural and dynamical properties of the two components near the surfaces are calculated and compared with the corresponding quantities in the bulk. The density profiles of the two components are found to be highly nonuniform in the interfacial region. The more polar component is found to be preferentially adsorbed at a charged surface whereas the reverse is true for an uncharged surface. This change of density with surface electric field is a nonlinear effect known as electrostriction. With increase of surface charge density, the more polar component exhibits a positive electrostriction and the less polar component shows a negative electrostriction. This electrostriction effect is found to play an important role in determining the dynamical properties of the interfaces. Pronounced orientational order is also found for the dipolar molecules which are seen to align perpendicular to a charged surface and parallel to an uncharged surface. However, no net polarization is found near an uncharged surface as expected. For charged surfaces, the polarization profiles reveal oscillations in the interfacial region indicating layering in the orientational structure. The orientational order of both kinds of molecules is found to change nonlinearly with composition and also with surface electric field.

For both the species, it is found that the perpendicular ($z$) diffusion near a surface is hindered and the lateral diffusion ($x,y$) is enhanced compared to diffusion in the bulk mixture. With increase of surface charge density, the perpendicular diffusion further decreases and the lateral diffusion increases. These changes occur in a nonlinear fashion. For the uncharged surfaces, the rotational diffusion is found to slow down near the surface for the pure liquid of the strongly polar component but an opposite behavior is observed when mixtures are formed by adding the weakly polar component. This varying rotational diffusional behavior originates from the combined effects of orientational ordering near the walls, incomplete solvation shell at the interfaces and selective adsorption of less polar molecules at the uncharged surfaces. For charged surfaces, the slowing down of rotational diffusion of interfacial molecules compared to that of bulk molecules is observed also for mixtures which can be attributed to the selective adsorption of more polar species at the charged surfaces. For all the systems, the rotational diffusion is found to decrease with increase of surface charge density in both interfacial and bulk regions. With increase of the mole fraction of the less polar species, the rotational diffusion of both the species increases for uncharged surfaces whereas it decreases for charged surfaces. This contrasting behavior can be attributed to an interplay between the dipole–dipole and dipole–surface interactions.

In this study, we considered a binary mixture of two components which differ widely in their polarity. Since our goal of the present study was to investigate the surface charge induced modifications of the interfacial structure and dynamics of a dipolar mixture of varying composition, the

sizes of the molecules are taken to be the same for simplicity. It will, however, be interesting to investigate the effects of unequal molecular sizes of the two components on the structure and dynamics of dipolar mixtures near charged surfaces.

The charged surfaces produce an unscreened uniform field in the present model interfacial systems. Such a situation can arise when dipolar solvents without any ions are kept in contact with charged electrodes. Such an unscreened electric field was also used in earlier studies of electric field effects on diffusion in water.[25] However, in many electrochemical situations and in charged membrane-solution systems, usually there are ions in the medium which screen the bare surface electrostatic field. Such screening effects can be incorporated either by using a screened electric field or by including the ions explicitly in the simulations. Since the present systems contain no ions to screen the surface electrostatic field, the solvent molecules become polarized in both interfacial and bulk regions. However, we note that the solvent density and polarization profiles and also the dynamical properties near the surfaces are not expected to change significantly when ions are present at very low concentration because in such cases the screening length would be much larger than the molecular diameter of solvent molecules. We note that the width of the contact interface is only one molecular diameter and that of the diffuse interface is about two molecular diameters. Thus, the present results of the interfacial structure and dynamics have relevance to systems having only dipolar solvents or dipolar solvents plus ions at very low concentration. Nevertheless, it would be interesting to simulate mixtures of solvent dipoles and ions near charged surfaces, especially at higher ion concentration. Work in these directions is in progress.

## ACKNOWLEDGMENT

The financial support of the Council of Scientific and Industrial Research (CSIR), Government of India, is gratefully acknowledged.

[1] J. N. Israelachvili, *Intermolecular and Surface Forces* (Academic, New York, 1992).
[2] M. F. Toney, J. N. Howard, J. Richer, G. L. Borges, D. G. Wiesler, D. Yee, and L. D. Sorensen, Nature (London) **368**, 444 (1994).
[3] M. F. Toney, J. N. Howard, J. Richer, G. L. Borges, J. G. Gordon, O. R. Melroy, D. G. Wiesler, D. Yee, and L. D. Sorensen, Surf. Sci. **335**, 326 (1995).
[4] K. Ataka, T. Yotsuyanagi, and M. Osawa, J. Phys. Chem. **100**, 10664 (1996).
[5] S.-B. Zhu and G. W. Robinson, J. Chem. Phys. **94**, 1403 (1991).
[6] X. Xia and M. L. Berkowitz, Phys. Rev. Lett. **74**, 3193 (1995); I-C. Yeh and M. L. Berkowitz, J. Chem. Phys. **112**, 10491 (2000).
[7] S. H. Lee, J. C. Rasaiah, and J. B. Hubbard, J. Chem. Phys. **85**, 5232 (1986); **86**, 2383 (1987).
[8] S. Senapati and A. Chandra, J. Mol. Struct.: THEOCHEM **455**, 1 (1998).
[9] A. A. Gardner and J. P. Valleau, J. Chem. Phys. **86**, 4171 (1987).
[10] G. M. Torrie, P. G. Kusalik, and G. N. Patey, J. Chem. Phys. **88**, 7826 (1988).
[11] G. M. Torrie, P. G. Kusalik, and G. N. Patey, J. Chem. Phys. **89**, 3285 (1988).
[12] V. Russier, J. Chem. Phys. **90**, 4491 (1989).
[13] M. J. Booth, D. Duh, and A. D. J. Haymet, J. Chem. Phys. **101**, 7925 (1994).
[14] R. Akiyama and F. Hirata, J. Chem. Phys. **108**, 4904 (1998).
[15] G. Rickayzen and M. J. Grimson, J. Chem. Soc., Faraday Trans. 2 **78**, 893 (1982).
[16] M. Moradi and G. Rickayzen, Mol. Phys. **68**, 903 (1989).
[17] P. Frodl and S. Dietrich, Phys. Rev. E **48**, 3741 (1993).
[18] C. E. Woodward and S. Nordholm, Mol. Phys. **60**, 415 (1987).
[19] C. E. Woodward and S. Nordholm, Mol. Phys. **60**, 441 (1987).
[20] C. N. Patra and S. K. Ghosh, J. Chem. Phys. **106**, 2752 (1997).
[21] D. Das, S. Senapati, and A. Chandra, J. Chem. Phys. **110**, 8129 (1999).
[22] A. Chandra, S. Senapati, and D. Sudha, J. Chem. Phys. **109**, 10439 (1998).
[23] H. J. C. Berendsen, J. R. Grigera, and T. P. Straatsma, J. Phys. Chem. **91**, 6269 (1987).
[24] P. G. Kusalik and I. M. Svishchev, Science **265**, 1219 (1994); I. M. Svishchev, P. G. Kusalik, J. Wang, and R. J. Boyd, J. Chem. Phys. **105**, 4742 (1996).
[25] M. Kiselev and K. Heinzinger, J. Chem. Phys. **105**, 650 (1996).
[26] S. Senapati and A. Chandra, J. Chem. Phys. **112**, 10467 (2000).
[27] S. Senapati and A. Chandra, J. Chem. Phys. **113**, 377 (2000).
[28] S. Senapati and A. Chandra, Chem. Phys. **242**, 353 (1999).
[29] C. Y. Lee, J. A. McCammon, and P. J. Rossky, J. Chem. Phys. **80**, 4448 (1984).
[30] L. Zhang, H. T. Davis, D. M. Kroll, and H. S. White, J. Phys. Chem. **99**, 2878 (1995).
[31] M. P. Allen and D. J. Tildesley, *Computer Simulation of Liquids* (Clarendon, London, 1987).
[32] J. Shelley and G. N. Patey, Mol. Phys. **88**, 385 (1996).
[33] S. Senapati and A. Chandra, Chem. Phys. **231**, 65 (1998).
[34] S. Senapati and A. Chandra, J. Chem. Phys. **111**, 1223 (1999).
[35] J. P. Hansen and I. R. McDonald, *Theory of Simple Liquids* (Academic, London, 1986).
[36] E. Spohr, Chem. Phys. **141**, 87 (1990).
[37] For example, for the equimolar mixture the perpendicular and parallel components of the translational diffusion coefficients of molecules in region II differ at the most by 15% from the corresponding bulk values. The rotational diffusion coefficients in the two regions are even closer, the difference in not more than 2% of the bulk values.